- 1 Determination of the Serum Concentrations of the Monoclonal Antibodies Bevacizumab,
- 2 Rituximab, and Panitumumab Using Porous Membranes Containing Immobilized Peptide
- 3 Mimotopes
- 4 Joshua D. Berwanger¹, Hui Yin Tan¹, Gia Jokhadze², and Merlin L. Bruening^{1,3*}
- ¹Department of Chemistry and Biochemistry, University of Notre Dame, Notre Dame, Indiana
- 6 46556, United States
- ²Takara Bio USA, Inc., Mountain View, California 94043, USA
- 8 ³Department of Chemical and Biomolecular Engineering, University of Notre Dame, Notre Dame,
- 9 Indiana 46556, United States
- *Corresponding author. mbruenin@nd.edu phone: +1 574-631-3024

11 Abstract

Effective monoclonal antibody (mAb) therapies require a threshold mAb concentration in patient 12 serum. Moreover, the serum concentration of the mAb Bevacizumab should reside in a specific 13 range to avoid side effects. Methods for conveniently determining the levels of mAbs in patient 14 sera could allow for personalized dosage schedules that lead to more successful treatments. This 15 work utilizes microporous nylon membranes functionalized with antibody-binding peptides to 16 capture Bevacizumab, Rituximab, or Panitumumab from diluted (25%) serum. Modification of 17 the capture peptide terminus is often crucial to create the affinity necessary for effective binding. 18 The high purity of eluted mAbs allows for their quantitation using native fluorescence, and 19 membranes are effective in spin devices that can be used in any laboratory. The technique is 20 21 effective over the therapeutic range of Bevacizumab concentrations. Future work aims at further modifications to develop rapid point-of-care devices and decrease detection limits. 22

Introduction

1

9

10

11

12

13

14

15

16

17

18

19

20

21

22

23

This paper describes fabrication of peptide-modified membranes that selectively bind the monoclonal antibodies (mAbs) Bevacizumab, Rituximab, or Panitumumab to enable determination of their concentrations. The important points in this research include showing the generality of peptide-based mAb capture in membranes; development of membranes for Bevacizumab analysis, as the effects of this antibody are particularly sensitive to its concentration; creation of a spin membrane format for mAb analysis; and demonstration of the importance of modifying peptide termini to create high affinities for target mAbs.

Monitoring of therapeutic mAb levels in blood is becoming increasingly important with the widespread adoption of these drugs. There are already more than 70 mAbs approved for therapeutic applications.^{1,2} As examples relevant to this work, physicians use Bevacizumab to treat certain types of brain tumors or some kidney, colorectal, lung, or breast cancers; Rituximab for autoimmune disease and lymphoma; and Panitumumab for treating colon cancer. 1,3-5 These highly versatile mAbs are among the best-selling drugs.⁶ Due to their high specificity, mAb treatments are often extraordinarily successful, but variations of mAb concentrations in patient sera may affect their efficacy. Prior studies indicate that the peak and trough concentrations of therapeutic mAbs in sera may vary 4- to 10-fold in patient populations at the same time point after injection. ^{7,8} In some cases, particularly for Bevacizumab, effective treatment depends on the mAb serum concentration, with high concentrations causing side effects and low concentrations resulting in ineffective treatments. ^{7,9,10} Development of methods that can rapidly quantify the therapeutic mAb concentration in patient serum could lead to personalized dosage regimens and avoid overprescribing of these very expensive treatments. A rapid mAb quantitation method could also prove useful when assessing pharmacokinetic profiles during drug development.¹¹

Current protocols for determining mAb concentrations include immunosorbent assays with optical detection, liquid chromatography/mass spectrometry analysis, or radiolabeling of antibodies. 7,11–15 These methods give accurate results, but they are costly and not amenable to monitoring in the clinic. The mass-spectrometry techniques require expensive equipment, whereas typical immunosorbent assays require primary and labelled secondary antibodies, and usually require multiple time-consuming steps. 16 Recently, multiplexed spatial or suspension-based assays have become more common for simultaneous measurement of multiple proteins. 17–19 Multiplexed assays are effective for identifying and quantifying many proteins in one sample, but the technique faces challenges with cross reactivity and non-specific binding of reagents, long assays times (~1 h), and often the need for specialized equipment. 20–23 Thus, a method requiring minimal time and few reagents would help to make therapeutic mAb quantitation more accessible.

This work functionalizes microporous membranes with mimotopes (epitope-mimicking peptides)²⁴ to rapidly isolate monoclonal antibodies from serum and facilitate subsequent analysis. Functionalized membranes are attractive in biocatalysis, protein separations, and mAb purification because short diffusion distances in the membrane pores expedite these processes.^{25–28} Prior studies immobilized mimotopes on quartz crystal microbalances or electrodes to quantify mAbs, but these devices suffer from interferences in serum.^{29–31} We previously immobilized a Trastuzumab-binding mimotope in nylon membranes to selectively capture this mAb.³² Here we extend the development of mimotope-containing membranes to selective capture of Rituximab, Bevacizumab, and Panitumumab. We selected these mAbs as test analytes because they are widely used in cancer and autoimmune disease treatment, and because previous papers provide peptide sequences that should bind to these antibodies.^{1,3} Notably, this study demonstrates that

- 1 modifications to the C- or N-terminus of the peptides are often important to increase the binding
- 2 affinity.³⁰ Additionally, we show that affinity constants for Bevacizumab binding are similar for
- 3 the free and immobilized mimotope. Bevacizumab-binding membranes may prove particularly
- 4 important because of the narrow therapeutic window for this antibody, and detection of the
- 5 native fluorescence of Bevacizumab enables its quantitation in the therapeutic range. Compared
- 6 to our prior study,³² the technical advances in this work include methods for selection and
- 7 development of three new epitope-mimicking peptides (an arduous task including terminus
- 8 modifications), the addition of spin membranes to make assays more convenient in lab use,³³
- 9 testing of the mimotope-modified membranes in sera from several patients, increasing the assay
- sensitivity, and monitoring of Bevacizumab at therapeutic levels.

Experimental Section

Materials

11

- Hydroxylated nylon (LoProdyne LP, Pall, 1.2 μm pore size, 110 μm thick) membranes
- were cleaned in a UV/O₃ chamber (Jelight, model 18) for 10 min prior to modification.
- 15 KGSGSGSWPRWLEN-NH₂ (Rit14, "-NH₂" indicates amidation of the C-terminus),
- 16 KGSGSGSWLEMHWPAHS (Bev1), WLEMHWPAHSGSGSGSK (Bev2), Acetyl-
- 17 WLEMHWPAHSGSGSGSK (Bev17), KGSGSGSDTDWVRMRDSAR (Pan1),
- 18 KGSGSGSDTDWVRMRDSAR-NH₂ (Pan19), and KGSGSGSQLGPYELWELSH (Tra19) were
- 19 synthesized by Genscript with a purity greater than 95%. Poly(acrylic acid) (PAA, average
- 20 molecular weight $\sim 100,000$ Da, 35% aqueous solution), polyethylenimine (PEI, branched, $M_w =$
- 21 25,000 Da), N-(3-dimethylaminopropyl)-N'-ethylcarbodiimide hydrochloride (EDC), N-
- 22 hydroxysuccinimide (NHS), Tween-20 surfactant, Tween-80 surfactant, D-(+)-trehalose
- 23 dihydrate, and human serum were used as received from Sigma-Aldrich. Deidentified patient

- serum samples were purchased from BioChemEd Services. Poly(vinyl) alcohol (PVA, 99–100 %
- 2 hydrolyzed, approximate molecular weight 8600 Da) was purchased from Acros Organic.
- 3 Trastuzumab (Genentech), Bevacizumab (Genentech), Rituximab (Genentech), and Panitumumab
- 4 (Amgen) were used from their therapeutic formulations. Buffers were prepared using analytical
- 5 grade chemicals and deionized water (Milli-Q, 18.2 M Ω cm).

Immobilization of Peptide Mimotopes in Porous Nylon Membranes

Membranes were modified with polyelectrolytes following published procedures that employ a peristaltic pump to flow solutions through the membranes at a rate of 1 mL/min. 32 After treatment of the nylon membranes with UV/O₃, 5 mL of 10 mM PAA (in 500 mM NaCl, pH 3, PAA concentration is that of the repeating unit) was circulated through the membrane for 20 min, and the membrane was washed with 10 mL of water. A 2 mg/mL solution of PEI (pH 3) was then circulated through the membrane for 20 min prior to washing with 10 mL of water. A subsequent layer of PAA was deposited on top of the PEI layer in the same manner as the first PAA layer. Activation of the membranes for peptide immobilization to the PAA/PEI/PAA film included circulating 10 mL of 0.1 M NHS, 0.1 M EDC through the membrane for 1 h and washing with 10 mL of water. Subsequently, 2 mL of a 1 mg/mL peptide solution in 0.1 M sodium carbonate (pH 9) was circulated through the membrane for 2 h prior to washing with 10 mL of water. For all modifications, the membranes had a surface area of 3.1 cm² based on an exposed diameter of 2 cm.

Breakthrough Curves and Adsorption Isotherms for mAb Capture in Peptide-Modified

Membranes

1 Using a peristaltic pump to flow solutions through the membranes at a rate of 1 mL/min, peptide-modified membranes were washed with 10 mL of 20 mM phosphate buffer (pH 7.4) 2 containing 300 mM NaCl (for Rit14-modfied membranes) or 150 mM NaCl (for Bev17- and 3 Pan19-modified membranes). To demonstrate membrane affinity and specificity, solutions 4 containing 0.05 mg/mL of Rituximab or 0.05 mg/mL of Trastuzumab in 20 mM phosphate buffer 5 (pH 7.4, 300 mM NaCl) were passed through Rit14-modified membranes, and the effluent 6 solutions were collected. This was repeated with solutions containing 0.05 mg/mL of 7 Bevacizumab or 0.05 mg/mL of Trastuzumab in 20 mM phosphate buffer (pH 7.4, 150 mM 8 9 NaCl) to test Bev17-modified membranes, and with 0.05 mg/mL of Panitumumab or 0.05 mg/mL of Trastuzumab in 20 mM phosphate buffer (pH 7.4, 150 mM NaCl) to test Pan19-10 modified membranes. Effluent aliquots were collected in three 4-drop intervals followed by two 11 5-drop intervals followed by two 1-minute intervals, and further aliquots were collected in 2-12 minute intervals until all solution had passed through the membrane using a flow rate of 0.5 13 mL/min. The collection tubes were weighed before and after solution collection to determine the 14 volume in each aliquot. The concentration of the effluent antibodies was determined using 15 fluorescence spectroscopy (Synergy H1 Microplate Reader) with calibration curves (mAb 16 standards from 0.00-0.05 mg/mL in binding buffer). The excitation wavelength was 270 nm, and 17 the wavelength of maximum emission was around 330 nm. Breakthrough curves were plotted as 18 the effluent concentration versus the total volume of loading solution passed through the 19 membrane, and the binding capacities were determined using the integral of the difference 20 between the feed and effluent concentrations in the breakthrough curves. After binding, 21 22 membranes were washed with 10 mL of wash buffer containing 20 mM, pH 7.4 phosphate buffer

- in 500 mM NaCl, and the amount of antibody in the wash was subtracted from binding in the
- 2 breakthrough curve to calculate the capacity.

The adsorption isotherms for Rituximab, Bevacizumab, and Panitumumab were determined from "equilibrium" binding capacities obtained from breakthrough curves at various feed mAb concentrations (0.005, 0.01, 0.02, 0.05, 0.1, 0.15, and 0.2 mg/mL) in 20 mM, pH 7.4 phosphate buffer. The buffer contained 300 mM NaCl for Rituximab binding and 150 mM NaCl for Bevacizumab and Panitumumab binding. (The 300 mM NaCl concentration during Rituximab binding decreased the levels of Rituximab detected during rinsing with 500 mM NaCl. For other mAbs, 150 mM NaCl was sufficient to give low mAb levels in the rinse. Experiments with diluted serum did not require 300 mM NaCl when binding Rituximab.) Experiments were repeated with three different membranes (diameters of ~2 cm) at each concentration.

Capture of mAbs from Human Serum for Gel Electrophoresis or Quantitation using

Fluorescence

Human serum (Sigma-Aldrich) was diluted 1:3 with phosphate buffer (20 mM phosphate, 150 mM NaCl, pH 7.4) and spiked with Rituximab, Bevacizumab or Panitumumab to a mAb concentration of 50 μg/mL. Subsequently, 500 μL of this spiked serum was passed at 0.1 mL/min through a stack of membranes with an exposed diameter of 1 cm. To capture essentially all of the antibody, the stacks contained 2 Rit14-modified membranes, 3 Bev17-modified membranes, or 3 Pan19-modified membranes. Prior to mAb capture, the stacks were washed with 8 mL of phosphate buffer (20 mM phosphate, 150 mM NaCl, pH 7.4). After mAb binding, the membrane stacks were washed with 20 mL of 20 mM phosphate buffer containing 500 mM NaCl, 0.5% polyvinyl alcohol (PVA), and 0.05% Tween-20, at 0.5 mL/min. The captured antibody was then eluted with three 600 μL aliquots of eluent (100 mM dithiothreitol with 2%, wt/v, sodium dodecyl

- sulfate) at 0.1 mL/min. Forty μL from each eluted aliquot was loaded into a 4-20% gradient SDS-
- 2 PAGE (polyacrylamide gel electrophoresis) gel. The supporting information describes the method
- 3 for analysis of eluates using liquid chromatography/mass spectrometry.
- 4 Studies to determine mAb serum concentrations based on the eluate fluorescence employed
- 5 a similar procedure. Human serum diluted 1:3 with phosphate buffer (20 mM phosphate, 150 mM
- 6 NaCl, pH 7.4) was spiked to concentrations of 0, 5, 10, 25, or 50 μg of a specific mAb per mL.
- 7 Also, a negative control experiment was run using 50 µg of the non-specific mAb Trastuzumab
- 8 spiked into the previously described dilute human serum, and the control was completed using
- 9 Bev17 membranes. Binding and elution occurred as described above, and the first two eluate
- aliquots were analyzed using fluorescence spectroscopy where the calibration curve used mAb
- standards prepared in the eluent. The third eluate aliquot contained minimal mAb.
- Since the pooled sera was heat treated, we decided to also heat treat the individual patient
- sera. The serum from individual patients was heat inactivated following the procedure suggested
- by Gemini Bio.³⁴ This was done for safety reasons and was performed before spiking the serum,
- so it should not affect the target mAb unless a denatured protein in the serum causes aggregation
- of the mAb. The patient serum was then diluted 1:3 with phosphate buffer (20 mM phosphate, 500
- 17 mM NaCl, pH 7.4) and was spiked with Bevacizumab to concentrations of 0, 25, 50, or 75 µg per
- mL. The binding, elution, and fluorescent quantitation followed the procedure described above.

Determination of mAb Concentrations Using Spin Membranes

- A Bev17-modified or Tra19-modified membrane was cut into discs with diameters of 0.7
- 21 cm, and 3 discs were stacked and mounted in a spin column at Takara Bio. Spin columns were
- first washed with 100 μ l of 20 mM phosphate, (150 mM NaCl, pH 7.4) at 350 x g for 30

- seconds. 200 μ L of Bevacizumab (5 50 μ g/mL) or 100 μ L of Trastuzumab (10 -120 μ g/mL) in
- 2 human serum diluted 1:7 (for Bevacizumab) or 1:3 (for Trastuzumab) with phosphate buffer (20
- 3 mM phosphate, 150 mM NaCl, pH 7.4) was loaded onto the spin column during centrifuging at
- 4 350 x g for 2 minutes. This was followed by 6 washes with 400 μL of 20 mM, pH 7.4 sodium
- 5 phosphate buffer containing 500 mM NaCl, 0.5 % (wt/v) PVA, 0.05 % (v/v) Tween-20, and then
- 6 4 washes with 400 μL of disodium hydrogen phosphate (0.13 M)-citric acid (0.037 M) buffer,
- 7 pH 6. Washes were done by centrifuging spin columns at 1200 x g for 1 minute. Finally, four
- 8 200 μl aliquots of 2 % (wt/v) SDS, 100 mM DTT were used to elute the spin columns at 1000 x
- 9 g for 1 min. The concentration of Bevacizumab or Trastuzumab in eluates was determined by
- measuring native fluorescence and comparing with a calibration curve prepared from
- Bevacizumab or Trastuzumab standards in the eluent. Three replicates using a new spin column
- for each Bevacizumab and Trastuzumab concentration spiked in diluted generic human serum
- 13 (Sigma-Aldrich) were carried out.

Results and Discussion

14

15

16

17

18

19

20

21

22

This section first characterizes the immobilization of mimotopes to PAA/PEI/PAA films in porous nylon membranes. Subsequently, we present breakthrough curves for mAb binding in buffers to determine values for binding capacities and affinity constants and demonstrate selectivities for the specific mAbs. Later subsections examine mAb capture from spiked serum. In those studies, determination of the fluorescence of membrane eluates allows determination of mAb concentrations. Finally, the last subsection describes the use of mAb-binding membranes in spin columns.

Mimotope Covalent Immobilization in Poly(acrylic acid)-containing Membranes

Mimotope linking to the membrane occurs via reaction of immobilized, activated PAA with amines at the lysine residues or amine termini of the mimotope peptides.³⁵ Prior reflectance infrared spectroscopy studies show that reaction of PAA with NHS leads to N-hydroxy succinimidyl esters that subsequently react with primary amine groups to form amide bonds. 32,36-To determine the amount of immobilized mimotope, we measured the fluorescence of the mimotope loading and rinsing solutions before and after passing them through the activated membrane. Calibration curves show that the fluorescence increases linearly with mimotope concentration (Figure S1, Figure numbers beginning with "S" refer to the supporting information). Based on these analyses, Table 1 shows the amount of immobilization for 6 different mimotopes. Binding capacities range from 30 to 50 mg of mimotope per mL of membrane. For Bevacizumab capture, the peptide with lysine at the N terminus (Bev1) shows more immobilization to PAA than the peptides with lysine at the C terminus (Bev2 or Bev17), but this may vary with the mimotope. In all cases, there is more than enough mimotope to bind mAbs. Given the high molecular mass of mAbs (~150 kDa) compared to the masses of the mimotopes (1560 to 2067 Da), even binding of 1 mAb per every 10 mimotopes would yield a binding capacity of 220-400 mg of mAb per mL membrane. In fact, the mAb binding capacity is less than 10 mg per mL of membrane (Table 1), so most immobilized peptides do not participate in mAb binding.

1

2

3

4

5

6

7

8

9

10

11

12

13

14

15

16

17

18

Table 1. Mimotope-immobilization capacities in activated PAA/PEI/PAA-modified nylon membranes, and subsequent mAb binding capacities.^a

Target mAb	Mimotope Sequence	Mimotope Binding Capacity (mg/mL)	mAb Binding Capacity (mg/mL)
Rituximab	KGSGSGSWPRWLEN-NH ₂ (Rit14)	43± 6	6.1±0.8
Bevacizumab	KGSGSGSWLEMHWPAHS (Bev1) WLEMHWPAHSGSGSGSK (Bev2) Acetyl-WLEMHWPAHSGSGSGSK (Bev17)	50±3 29±2 28±4	0.3±0.1 1.2±0.5 6.0±0.3
Panitumumab	KGSGSGSDTDWVRMRDSAR (Pan1) KGSGSGSDTDWVRMRDSAR-NH ₂ (Pan19)	49±4 40±3	1.1±0.3 4.8±1.0

^amAb binding capacities were determined using a 0.05 mg/mL feed concentration.

Selection of Mimotopes and their Immobilization Chemistry

mAb binding to immobilized peptide mimotopes depends on the peptide composition and terminus modifications. We selected initial mimotopes based on literature reports of phage-display or mRNA-display screening of specific peptide sequences. ^{30,39–41} In these processes, libraries of peptides are initially displayed either on the surface of a bacteriophage or fused to their own mRNA sequences. Peptides are then selected based on their affinity for their target mAbs (Rituximab, Bevacizumab, and Panitumumab), and the selected smaller peptide library is subsequently amplified. Repetition of the process occurs until a few peptides with high affinity for the target result. ^{42–47} Based on the previously discovered peptides, we selected amino-acid sequences with a binding region containing as few amino acids as possible to decrease the cost of synthesis while also displaying high affinity to the target mAb to ensure specific binding. The

- 1 peptides we designed also contain a hydrophilic linking sequence (GSGSGS)²⁹ and a terminal
- 2 lysine to enhance immobilization.

- Prior studies suggest that blocking the peptide termini (via acetylation of the N-terminus or amidation of the C-terminus) to remove charged amine and carboxylate groups at these termini is sometimes useful for mimicking the native epitope, which is part of a larger protein sequence.⁴⁸ For a mimotope analogous to Rit14, amidation of the C-terminus increased the affinity and selectivity for Rituximab binding to a mimotope-modified Au surface. ³⁰ Those results led us to use the C-terminally amidated Rituximab mimotope in our work. Additionally, when developing Pan19, the Panitumumab binding capacity increased over 4-fold when using a mimotope with C-terminal amidation (compare Pan19 and Pan1 in Table 1).
 - We investigated three different peptides, KGSGSGSWLEMHWPAHS (Bev1), WLEMHWPAHSGSGSGSK (Bev2), and Acetyl-WLEMHWPAHSGSGSGSK (Bev17), in the search for an effective Bevacizumab-binding mimotope. The first two peptides have the linker and lysine residue on opposite ends of the affinity sequence, WLEMHWPAHS.³⁹ The last peptide has N-terminal acetylation to confine immobilization to the peptide C-terminus. All three sequences allowed successful mimotope immobilization in membranes (Table 1), but Bev17 captured the most Bevacizumab. Although Bev1 showed the highest amount of mimotope immobilization, the Bevacizumab binding capacity was only 0.3±0.1 mg of Bevacizumab per mL of membrane. Compared to Bev1, Bev2 gave a 40% decrease in mimotope immobilization while also having four times the Bevacizumab binding capacity. This binding capacity was still low, so we purchased the N-terminal acetylated peptide, Bev17, in hopes of increasing Bevacizumab capture. Fortunately, this led to a 5-fold increase in the Bevacizumab binding capacity with a similar amount of mimotope immobilization as Bev2 (Table 1).

Selective Therapeutic mAb Capture Using Mimotope-functionalized Membranes

Rit14, Bev17, and Pan19 are mimotopes
for the antigens of Rituximab, Bevacizumab,
and Panitumumab, respectively, so membranes
functionalized with these mimotopes should
selectively capture these specific mAbs. We
first obtained breakthrough curves using 0.05
mg/mL antibody solutions in buffer to

investigate the binding capacity of each

mimotope-containing membrane. Separate

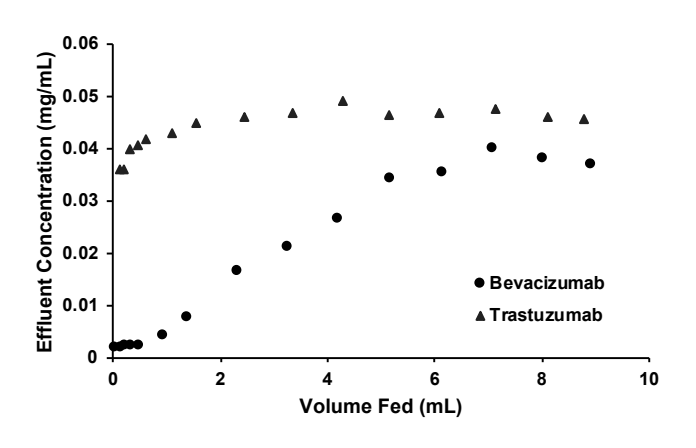


Figure 1. Breakthrough Curves for Bevacizumab or Trastuzumab passing through a Bev17-modified membrane. The feed concentration for both mAbs was 0.05 mg/mL, and the membrane area was 3.1 cm².

breakthrough curves indicate negligible binding of a non-target mAb, Trastuzumab, showing that the mimotopes have selectivity for the Fab region of the humanized target antibody versus the humanized Fc region or Fab region of another mAb. Figure 1 shows breakthrough curves for Bev17-functionalized membranes, and Figures S2A and S2B present similar curves for Rit14- and Pan19-modified membranes. All of the membranes capture <1 mg of Trastuzumab per mL of membrane, and even some of this "binding" in the first mL is likely due to the dead volume in the system and a small amount of nonspecific adsorption, which should decrease in the presence of other proteins in serum. As Figure 1 shows, the Bev17-functionalized membrane captures nearly all of the Bevacizumab in the first mL of solution passed through the membrane and >80% of Bevacizumab in the first 2 mL of solution. The "equilibrium" binding capacity at this antibody concentration is 6.0±0.3 mg of Bevacizumab per mL of membrane. Similarly, Rit14-modified membranes capture 6.1±0.8 mg of Rituximab per mL of membrane at "equilibrium" (Figure S2A) and Pan19-functionalized membranes bind 4.8±1.0 mg of Panitumumab per mL of

- 1 membrane (Figure S2B). Note that these binding capacities are less than the true equilibrium
- 2 binding capacity because the permeate concentration never completely reaches the feed
- 3 concentration. Binding sites in narrow pores in the membrane likely fill slowly. Hence the
- 4 binding capacities represent "equilibrium" only with readily accessible sites, which are most
- 5 useful for mAb capture. In all the breakthrough experiments, we limited the feed volume to 9
- 6 mL. The use of larger volumes will introduce significant errors due to the uncertainties in the
- 7 small differences in feed and effluent concentrations as the membrane approaches true
- 8 "equilibrium".

10

11

13

14

15

16

17

18

19

20

21

22

23

Adsorption Isotherms and Comparison to Binding in Solution

After demonstrating a reasonable binding capacity and specificity, we determined "equilibrium" binding capacities at different feed concentrations to develop adsorption isotherms

for different membranes. Figure 2 shows the

concentration-dependent Bevacizumab binding

capacity for Bev17-modified membranes along with

the Langmuir adsorption isotherm fit to the data.

Figures S3A and S3B present the corresponding

figures for specific mAb adsorption in Rit14- and

Pan19-modified membranes. Equation 1 describes

two equivalent forms of the Langmuir isotherm,

where q is the equilibrium binding capacity at a

given mAb feed concentration, q_0 is the saturation

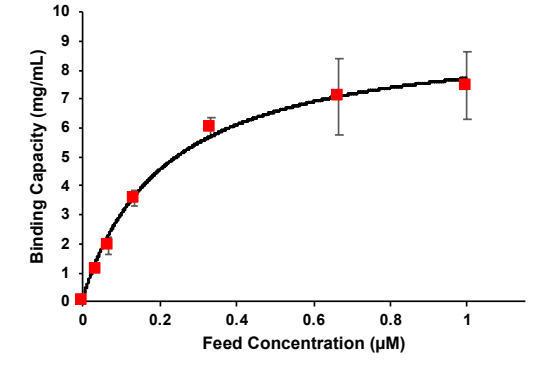


Figure 2. Adsorption isotherm for Bevacizumab binding to Bev17-modified membranes. The curve shows the best fit of the data to the Langmuir adsorption isotherm, and error bars are the standard deviations of capacities from breakthrough curves on three different membranes. A 1 μ M solution is equivalent to \sim 0.15 mg/mL of antibody.

binding capacity, K_a is the association constant, K_d is the dissociation constant and [mAb] is the

equilibrium concentration of the target mAb. 49,50

$$q = q_0 \frac{K_a[mAb]}{1 + K_a[mAb]} = q_0 \frac{[mAb]}{K_d + [mAb]}$$
 (1)

Table 2 presents the fitted values of q_0 and K_d . The Bev17-functionalized membrane shows a q_0 value of 9.2 mg of Bevacizumab per mL of membrane, and a K_d value of 215 nM (association constant, $K_a = 1/K_d$, of 4.6 x 10^6 M⁻¹). The Rit14-modified membranes have the highest value of q_0 (16.5 mg of Rituximab per mL of membrane), whereas saturation binding capacities for Bev17- and Pan19-functionalized membranes are 9-10 mg/mL. These q_0 values correspond to capture of \sim 4 x 10^{14} target antibody molecules per cm² of external surface area. In contrast, q_0 for a nonporous well whose base has an area of 1 cm² is at most 1.3 x 10^{12} antibodies. The high internal surface area of the membrane leads to a binding capacity that is several orders of magnitude greater than that for a similar-sized well. The K_d values are 0.2-0.4 μ M for all three modified membranes binding to their target antibodies, and typical ELISAs exploit K_d values between 10^{-5} and 10^{-12} M for antibodies binding to their target antigens. $^{51-57}$

Table 2. Dissociation constants for antibody binding to mimotope-modified membranes (K_d from the Langmuir Isotherm) or free mimotopes (K_d from isothermal titration calorimetry, ITC), and saturation binding capacities (q_0) for antibody binding to mimotope-modified membranes.

Target mAb	Mimotope	Langmuir Isotherm K _d (µM)	$q_0 \ (ext{mg/mL})$	ITC K _d (μM)
Rituximab	Rit14	0.49±0.11	16.5	16.1±0.4
Bevacizumab	Bev17	0.22±0.04	9.2	0.35 ± 0.06
	Bev1 ^a	-	-	Not Detectable
	Bev2 ^a	-	-	Not Detectable
Panitumumab	Pan19	0.44±0.11	9.8	16±2
	Pan1 ^a	-	-	Not Detectable

^aBreakthrough curves at a single concentration showed minimal binding (Table 1).

3 To find out whether peptide immobilization alters binding affinity, we also determined dissociation constants for complexes of peptides and mAbs in solution (Figures S4 and S5 show 4 the calorimetry data). Using isothermal titration calorimetry (ITC),⁵⁸ we obtained the 5 dissociation constants listed in Table 2. For Rit14 and Pan19, the K_d was larger in solution than 6 7 in the membranes, suggesting that peptide immobilization may increase affinity. Perhaps, the 8 bivalent antibody binds to two immobilized mimotopes that are in close proximity, thus increasing the antibody's affinity for the membrane. ^{59–61} The dissociation constant for free 9 Bev17 is similar to that for the immobilized peptide. The Bev17 peptide had 30-35% less 10 11 immobilization than Rit14 and Pan19, which could explain why the affinity in solution and in the 12 membrane were similar. Additionally, peptides that showed low mAb binding when immobilized in membranes (see Table 1) also showed no detectable binding in solution. 13

Selective binding of target mAbs from serum

Experiments with mAb binding from diluted (1:3) human serum (pooled serum from Sigma-Aldrich) demonstrate selective capture from solutions containing a large excess of other proteins, including other antibodies. To visually demonstrate selective binding, we performed gel electrophoresis of the spiked serum (before and after passing through the membrane) and the antibody-containing eluate. Figure 3 shows the SDS-PAGE analysis of Bevacizumab capture in a Bev17-functionalized membrane, and Figures S6A and S6B are images of corresponding gels for mAb capture in Rit14- and Pan19-modified

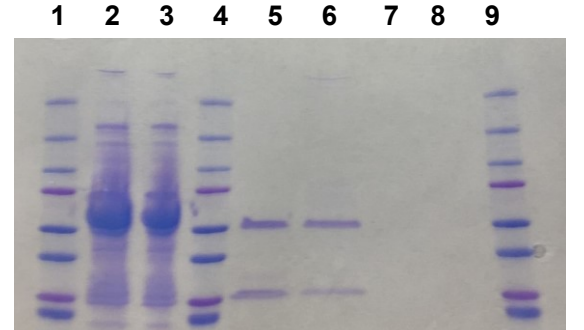


Figure 3. SDS PAGE analysis of Bevacizumab capture (from serum) and elution in Bev17-modified membranes. Lanes 1,4, and 9 contain the molecular weight ladder. Lanes 2 and 3 show protein from the spiked feed (25% serum) and effluent solutions after a 10-fold dilution. Lane 5 is a Bevacizumab standard (1.25 μg), and lanes 6-8 are the eluted protein in 30 μL (each) from 3 consecutive 0.6-mL eluate aliquots. The membrane was loaded with 0.5 mL of 25% serum containing 0.05 mg/mL Bevacizumab.

membranes, respectively. In these figures, the lane containing the spiked serum shows a high abundance of many proteins. In contrast, lane 6 which contains protein from the first eluate aliquot shows dominant bands that appear around 25 and 50 kDa and correspond to the target antibody light and heavy chains, respectively. Nearly all of the captured mAb elutes in the first eluate aliquot, and the dominance of the antibody bands shows that the eluted samples are relatively pure. The similar intensities of antibody bands in lanes 5 and 6 suggest high recovery of the antibody from serum, as lane 5 contains the amount of antibody corresponding to 100% recovery. Control experiments that examined protein binding from unspiked diluted (1:3) serum did not show bands corresponding to antibody light and heavy chains (Figure S7) or any other significant bands, implying low amounts of non-specific binding or binding of other antibodies in serum.

LC/MS data confirm that the eluted protein is highly pure. Figure 4 shows the chromatogram of Bevacizumab eluted from a membrane that was loaded with 0.05 mg/mL Bevacizumab in 1:3 diluted serum. The chromatogram contains two dominant peaks, and MS spectra show that these peaks correspond to the light and heavy

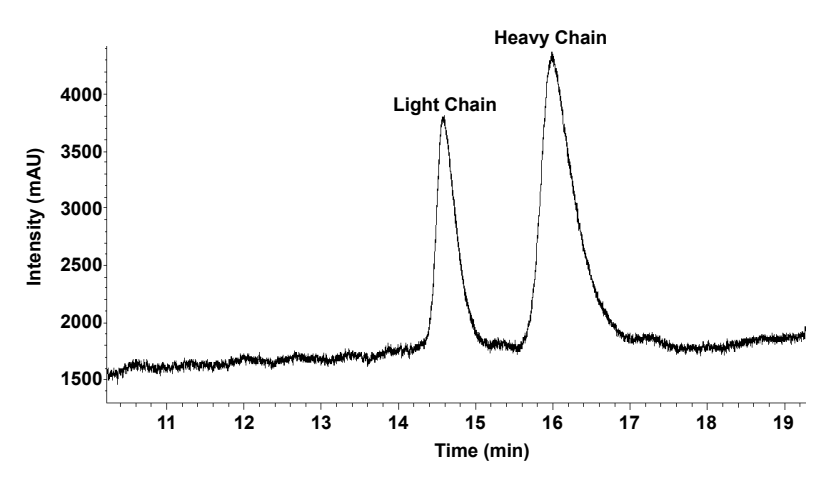


Figure 4. Liquid chromatogram (UV detection at 280 nm) of the eluate from a Bev17-modified membrane. MS spectra show a deconvoluted mass of 23451.88 Da for the first peak (36 ppm difference from the Bevacizumab light chain) and 51166.34 Da for the second peak (58 ppm mass difference from the G0F glycan of the heavy chain) to identify the eluted antibody as Bevacizumab.

chains of Bevacizumab (see Figure S8 in the supporting information).

Target mAb quantitation in human serum

The above results demonstrate selective capture of specific mAbs and their subsequent elution. This section examines whether capture and elution are sufficiently reproducible to enable determination of mAb concentrations based on the native antibody fluorescence of eluate solutions.

Specifically, we passed 0.5 mL of mAb-spiked serum (diluted 1:3 with buffer) through a membrane stack, rinsed the system, eluted with three 0.6-mL aliquots of eluent and determined the fluorescence intensity of the eluate solutions. Based on the breakthrough

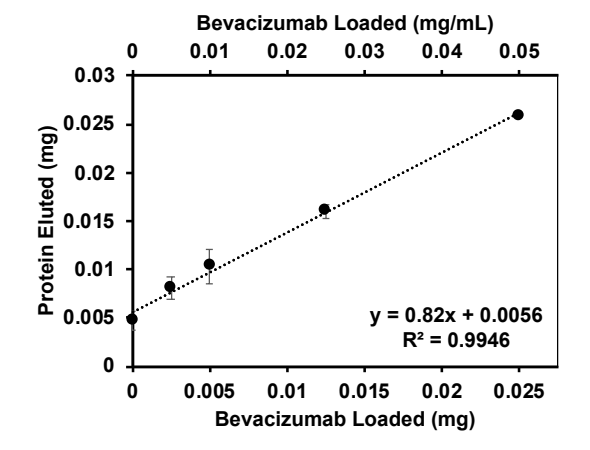


Figure 5. Total Protein Eluted from membranes loaded with serum spiked with different concentrations of Bevacizumab. The total protein was quantified by determining the fluorescence of the eluates compared to Bevacizumab standards made in the elution buffer. Error bars represent the standard deviation of three replicate experiments on three different membrane stacks.

1 curves, use of the limited loading volume (0.5 mL) should lead to nearly complete capture of the

mAb in the membrane stack, and the large eluate volume should elute essentially all of the bound

mAb.

As Figure 5 shows, the slope in the plot of Bevacizumab recovered in the eluate versus the amount of loaded Bevacizumab is 0.82 ± 0.02 , suggesting that total recovery of mAb is ~80%, although the percent recovery was only around 60% with a second batch of the peptide mimotope, so calibration is necessary with each batch of membranes. Rituximab analysis with Rit14-modified membranes gave a similar slope of 0.84 ± 0.10 (See Figure S9A), but the slope for Panitumumab analysis was only 0.23 ± 0.02 (Figure S9B), although all three plots are linear. The responses plateau at concentrations greater than 0.05 mg/mL for Bevacizumab and Rituximab or 0.1 mg/mL for Panitumumab as the membrane approaches saturation. The low Panitumumab recovery may suggest interaction of the mAb with other proteins in serum.

The plot in Figure 5 and the corresponding plots for the other antibodies all show a non-zero y-intercept around 0.006 mg. This likely corresponds to the fluorescence of non-specifically adsorbed protein that subsequently elutes in the SDS/DTT solution. We tried extensive washing with buffers containing high salt and surfactant concentrations, but the low level of non-specific binding persisted. Fortunately, the level of non-specific binding is consistent, so one can correct for it in the calibration curve. As a negative control, we also analyzed diluted serum spiked with 0.05 mg/mL of Trastuzumab on the Bev17 membrane. The amount of protein eluted was 0.006±0.001 mg, essentially the same as the non-specific binding observed with unspiked diluted serum. A membrane with a non-target mimotope could serve as a negative control if needed.

The standard curve in Figure 5 could potentially prove useful in determining

Bevacizumab concentrations in patient sera. Bevacizumab has a narrow therapeutic window

(0.2-0.25 mg per mL of serum),⁷ and our curve effectively quantifies Bevacizumab below this

range (0.005-0.05 mg per mL of serum). Thus, a 1:9 dilution of serum will put the desired

Bevacizumab level in the middle of the calibration curve, and this will decrease the amount of

patient serum necessary for quantitation. The further dilution may also decrease the amount of

non-specific binding to increase the precision of the measurement.

We then tested the Bev17-based analysis method using sera from different patients rather than the pooled serum from Sigma-Aldrich. These experiments examined spiked-Bevacizumab capture from the sera of four different unidentified patients (2 males and 2 females). The amount of protein eluted increases with the amount of Bevacizumab loaded for all four of the patient sera (Figure S10). Figure 6 presents the combined data from analyses of all four patient sera and

shows a linear response with a slope of 0.46±0.03. This suggests a Bevacizumab recovery of ~46% with these membranes, which is less than in the initial studies with the serum from Sigma-Aldrich. This shows the need for calibration. We suspect that the recoveries differ in part due to different heat-treatment or other treatment of the sera. Differences in pretreatment could leave more aggregated proteins in the patient serum. Additionally, we also added more salt to the dilution buffer (0.5 M NaCl) for the patient samples than for the pooled serum (0.15 M NaCl) in

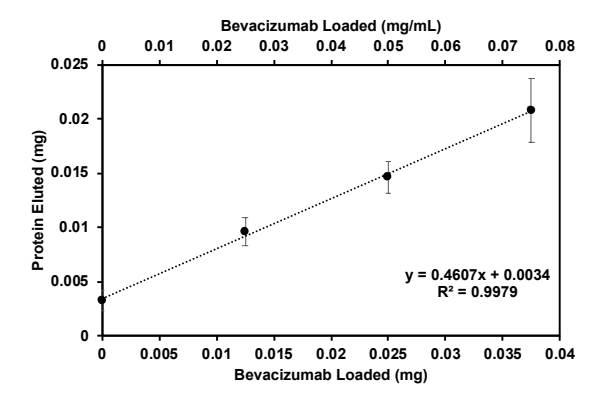


Figure 6. Total Protein Eluted from membranes loaded with Bevacizumab-spiked sera from four different patients. The total protein was quantified by determining the fluorescence of the eluates compared to Bevacizumab standards made in the elution buffer. Error bars represent the 95 % confidence interval of 12 replicate experiments (replicates on three different membrane stacks for each of the four patients.)

an effort to decrease non-specific binding. The lower recovery observed in patient samples also

2 suggests that there might be a matrix effect, which could vary among a large number of patients.

3 One possibility for overcoming this challenge is to further dilute the serum. The y-intercept in

4 Figure 6 is 0.0034 mg which is about 40 percent lower than the intercept for the Sigma-Aldrich

5 serum. Regardless of the differences between patient and commercial serum, there is little

6 variance in the data when comparing patients. An ANOVA two-way test comparing analyses of

the four patients' sera spiked with the four feed concentrations gave no statistically significant

variance in the observed data due to the different patients' sera (Supporting Information section

9 S11).

The Rit14 and Pan19 analyses based on eluate fluorescence are not sufficient for therapeutic monitoring because the levels in serum are typically above 0.025 mg/mL for Rituximab and between 0.0213 and 0.039 mg/mL for Panitumumab. 62.63 After serum dilution, the assay would not be sufficiently sensitive. However, the method might prove useful for quantitation of these drugs during production. After proper dilution, broths could be passed through the membranes, washed, eluted, and quantified with fluorescence to rapidly determine batch concentrations. Though our native fluorescence detection method is a few orders of magnitude less sensitive than ELISA methods, we are working to achieve more selective and sensitive detection methods employing labelled secondary antibodies. Figure S11 suggests that the use of fluorescently labelled secondary antibodies may decrease detection limits several orders of magnitude. The increased sensitivity of the assay shown in Figure S11 will allow for further dilution of patient samples in the future, which may help to overcome possible matrix effects that vary among patients. Such membrane-based methods may compete with the sensitivities of ELISA while providing data in less than a third of the time. 64-66

mAb quantitation using spin membranes

The setup used in the above experiments requires pumping of solutions through membranes, which some labs may consider cumbersome and labor-intensive. To make the process more amenable to a typical biochemistry lab, we embedded membranes in spin filters and performed the loading, rinsing, and elution steps using centrifugation. As Figure S12 shows, the Bevacizumab calibration curve is similar for the spin membranes and the peristaltic pump device. Passing loading, rinsing, and eluate solutions through the membrane requires about 50 min with the peristaltic pump and 20 min with the spin device. Thus, the spin device may prove more convenient. Moreover, we are working on decreasing rinsing times to decrease analysis times by a factor of two.

This paper shows some of the promise of the membrane-based mAb capture and analysis, and current work is focusing on incorporation of such membranes into microfluidic devices. In addition to extensive clinical testing, which is beyond the scope of this work, development of a membrane-based point-of-care device will likely require incorporation of the membranes in a microfluidic system to work with less volume and shorten assay time. Preliminary data suggest that binding of fluorescent secondary antibodies directly to the membrane can decrease detection limits several orders of magnitude (see Figure S11).

Conclusions

We previously demonstrated modification of porous nylon membranes through immobilization of peptide mimotopes to adsorbed poly(acrylic acid) and showed that these membranes selectively capture the therapeutic mAb Trastuzumab.³² This work expands the range of mimotopes to capture three additional mAbs and specifically develops a method for analysis

- of Bevacizumab, which has a very narrow therapeutic window. Remarkably, immobilization of
- 2 Bev17 had minimal effect on its affinity for Bevacizumab compared to binding to the free
- 3 mimotope in solution. However, affinity for a given mAb sometimes increases after acetylating
- 4 or amidating the mimotope peptide terminus. Spin membranes may make the process for
- 5 capturing, rinsing, and eluting mAbs from membranes more convenient, and determination of the
- 6 fluorescence of eluate solutions allows analysis of Bevacizumab concentrations in their
- 7 appropriate therapeutic window. Nevertheless, future work should examine methods for
- 8 incorporating membranes in automated point-of-care devices with simpler workflows and
- 9 detection methods.⁶⁷

Acknowledgment

- We are grateful to the National Science Foundation (CHE1903967) for partial funding of this
- work. We also acknowledge funding from the NSF IUCRC Center for Bioanalytical Metrology
- 13 (1916601).

10

14 Supporting Information

- 15 The supporting information is available free of charge on the ACS Publication Website at
- 16 DOI:XXX.
- 17 Fluorescence spectra of Rit14, Bev17, and Pan19 for quantifying mimotope immobilization;
- Breakthrough curves for Rit14- and Pan19-modified Membranes; Adsorption isotherms for
- 19 Rit14- and Pan19-modified membranes; Isothermal Titration Calorimetry; SDS PAGE analysis
- of mAb capture and elution in Rit14- and Pan19-modified membranes; Calibration curves for
- 21 mAbs eluted from membranes; ANOVA two-way test of analyses with sera from various

- patients; Calibration curves for mAbs eluted from Bev17- and Tra17-modified *spin* membranes;
- 2 Procedures for LC/MS analysis of eluted proteins.

2 References

1

Singh, S.; Tank, N. K.; Dwiwedi, P.; Charan, J.; Kaur, R.; Sidhu, P.; Chugh, V. K.
 Monoclonal Antibodies: A Review. *Curr. Clin. Pharmacol.* 2018, *13* (2), 85–99.
 https://doi.org/10.2174/1574884712666170809124728.

- 6 (2) Lu, R.-M.; Hwang, Y.-C.; Liu, I.-J.; Lee, C.-C.; Tsai, H.-Z.; Li, H.-J.; Wu, H.-C.
 7 Development of Therapeutic Antibodies for the Treatment of Diseases. *J. Biomed. Sci.* 8 2020, 27 (1), 1. https://doi.org/10.1186/s12929-019-0592-z.
- 9 (3) Berger, M.; Shankar, V.; Vafai, A. Therapeutic Applications of Monoclonal Antibodies. 10 Am. J. Med. Sci. 2002, 324 (1), 14–30. https://doi.org/10.1097/00000441-200207000-11 00004.
- 12 (4) Vectibix (Panitumumab Injection for Intravenous Use): Side Effects, Interactions,
 13 Warning, Dosage & Uses https://www.rxlist.com/vectibix-drug.htm (accessed Nov 1,
 14 2019).
- 15 (5) Avastin (Bevacizumab): Uses, Dosage, Side Effects, Interactions, Warning https://www.rxlist.com/avastin-drug.htm (accessed Mar 8, 2021).
- 17 (6) The Top 15 Best-Selling Drugs of 2016 | The Lists | GEN Genetic Engineering & Biotechnology News Biotech from Bench to Business http://www.genengnews.com/the-lists/the-top-15-best-selling-drugs-of-2016/77900868 (accessed Jul 19, 2017).
- Nugue, G.; Bidart, M.; Arlotto, M.; Mousseau, M.; Berger, F.; Pelletier, L. Monitoring
 Monoclonal Antibody Delivery in Oncology: The Example of Bevacizumab. *PLOS ONE* 2013, 8 (8), e72021. https://doi.org/10.1371/journal.pone.0072021.
- Baselga, J.; Carbonell, X.; Castañeda-Soto, N.-J.; Clemens, M.; Green, M.; Harvey, V.;
 Morales, S.; Barton, C.; Ghahramani, P. Phase II Study of Efficacy, Safety, and
 Pharmacokinetics of Trastuzumab Monotherapy Administered on a 3-Weekly Schedule. *J. Clin. Oncol.* **2005**, *23* (10), 2162–2171. https://doi.org/10.1200/JCO.2005.01.014.
- 27 (9) Berinstein, N. L.; Grillo-López, A. J.; White, C. A.; Bence-Bruckler, I.; Maloney, D.;
 28 Czuczman, M.; Green, D.; Rosenberg, J.; McLaughlin, P.; Shen, D. Association of Serum
 29 Rituximab (IDEC-C2B8) Concentration and Anti-Tumor Response in the Treatment of
 30 Recurrent Low-Grade or Follicular Non-Hodgkin's Lymphoma. *Ann. Oncol. Off. J. Eur.*31 Soc. Med. Oncol. 1998, 9 (9), 995–1001. https://doi.org/10.1023/A:1008416911099.
- Widmer, N.; Bardin, C.; Chatelut, E.; Paci, A.; Beijnen, J.; Levêque, D.; Veal, G.; Astier,
 A. Review of Therapeutic Drug Monitoring of Anticancer Drugs Part Two--Targeted
 Therapies. Eur. J. Cancer Oxf. Engl. 1990 2014, 50 (12), 2020–2036.
 https://doi.org/10.1016/j.ejca.2014.04.015.
- Ovacik, M.; Lin, K. Tutorial on Monoclonal Antibody Pharmacokinetics and Its Considerations in Early Development. *Clin. Transl. Sci.* **2018**, *11* (6), 540–552. https://doi.org/10.1111/cts.12567.
- Fischer, S. K.; Yang, J.; Anand, B.; Cowan, K.; Hendricks, R.; Li, J.; Nakamura, G.; Song,
 A. The Assay Design Used for Measurement of Therapeutic Antibody Concentrations Can
 Affect Pharmacokinetic Parameters: Case Studies. *mAbs* 2012, 4 (5), 623–631.
 https://doi.org/10.4161/mabs.20814.
- 43 (13) Wilffert, D.; Bischoff, R.; van de Merbel, N. C. Antibody-Free Workflows for Protein Quantification by LC-MS/MS. *Bioanalysis* **2015**, 7 (6), 763–779. https://doi.org/10.4155/bio.14.308.

- 1 (14) Avery, L. B.; Wang, M.; Kavosi, M. S.; Joyce, A.; Kurz, J. C.; Fan, Y.-Y.; Dowty, M. E.; Zhang, M.; Zhang, Y.; Cheng, A.; Hua, F.; Jones, H. M.; Neubert, H.; Polzer, R. J.;
- O'Hara, D. M. Utility of a Human FcRn Transgenic Mouse Model in Drug Discovery for Early Assessment and Prediction of Human Pharmacokinetics of Monoclonal Antibodies.
- 5 *mAbs* **2016**, 8 (6), 1064–1078. https://doi.org/10.1080/19420862.2016.1193660.
- (15) Iwamoto, N.; Umino, Y.; Aoki, C.; Yamane, N.; Hamada, A.; Shimada, T. Fully Validated
 LCMS Bioanalysis of Bevacizumab in Human Plasma Using Nano-Surface and
 Molecular-Orientation Limited (NSMOL) Proteolysis. *Drug Metab. Pharmacokinet.* 2016,
 31 (1), 46–50. https://doi.org/10.1016/j.dmpk.2015.11.004.
- (16) Hosseini, S.; Vázquez-Villegas, P.; Rito-Palomares, M.; Martinez-Chapa, S. O.
 Advantages, Disadvantages and Modifications of Conventional ELISA. In *Enzyme-linked Immunosorbent Assay (ELISA): From A to Z*; Hosseini, S., Vázquez-Villegas, P., Rito-Palomares, M., Martinez-Chapa, S. O., Eds.; SpringerBriefs in Applied Sciences and Technology; Springer Singapore: Singapore, 2018; pp 67–115.
 https://doi.org/10.1007/978-981-10-6766-2 5.
- 16 (17) Elshal, M. F.; McCoy, J. P. Multiplex Bead Array Assays: Performance Evaluation and Comparison of Sensitivity to ELISA. *Methods San Diego Calif* **2006**, *38* (4), 317–323. https://doi.org/10.1016/j.ymeth.2005.11.010.
- 19 (18) Leng, Y.; Sun, K.; Chen, X.; Li, W. Suspension Arrays Based on Nanoparticle-Encoded
 20 Microspheres for High-Throughput Multiplexed Detection. *Chem. Soc. Rev.* **2015**, *44* (15),
 21 5552–5595. https://doi.org/10.1039/C4CS00382A.
- (19) Wilson, R.; Cossins, A. R.; Spiller, D. G. Encoded Microcarriers For High-Throughput
 Multiplexed Detection. *Angew. Chem. Int. Ed.* 2006, 45 (37), 6104–6117.
 https://doi.org/10.1002/anie.200600288.
- (20) Cohen, L.; Walt, D. R. Highly Sensitive and Multiplexed Protein Measurements. *Chem. Rev.* 2019, *119* (1), 293–321. https://doi.org/10.1021/acs.chemrev.8b00257.
- Juncker, D.; Bergeron, S.; Laforte, V.; Li, H. Cross-Reactivity in Antibody Microarrays and Multiplexed Sandwich Assays: Shedding Light on the Dark Side of Multiplexing.
 Curr. Opin. Chem. Biol. 2014, 18, 29–37. https://doi.org/10.1016/j.cbpa.2013.11.012.
- 30 (22) How to Run an R&D Systems Luminex® Assay
 31 https://www.rndsystems.com/resources/protocols/how-run-rd-systems-luminex-assay
 32 (accessed Jan 25, 2021).
- 33 (23) A review of current multiplex immunoassay methods | Abcam 34 https://www.abcam.com/kits/multiplex-immunoassay-techniques-review-of-methods-35 western-blot-elisa-microarray-and-luminex (accessed Feb 23, 2021).
- 36 (24) Geysen, H. M.; Rodda, S. J.; Mason, T. J. A Priori Delineation of a Peptide Which Mimics
 37 a Discontinuous Antigenic Determinant. *Mol. Immunol.* 1986, 23 (7), 709–715.
 38 https://doi.org/10.1016/0161-5890(86)90081-7.
- Wang, J.; Jenkins, E. W.; Robinson, J. R.; Wilson, A.; Husson, S. M. A New Multimodal
 Membrane Adsorber for Monoclonal Antibody Purifications. *J. Membr. Sci.* 2015, 492,
 137–146. https://doi.org/10.1016/j.memsci.2015.05.013.
- (26) Sarma, R.; Islam, Md. S.; Miller, A.-F.; Bhattacharyya, D. Layer-by-Layer-Assembled
 Laccase Enzyme on Stimuli-Responsive Membranes for Chloro-Organics Degradation.
 ACS Appl. Mater. Interfaces 2017, 9 (17), 14858–14867.
- 45 https://doi.org/10.1021/acsami.7b01999.

- 1 (27) Keating, J. J.; Imbrogno, J.; Belfort, G. Polymer Brushes for Membrane Separations: A Review. *ACS Appl. Mater. Interfaces* **2016**, *8* (42), 28383–28399. https://doi.org/10.1021/acsami.6b09068.
- (28) Liu, D.; Ulbricht, M. A Highly Selective Protein Adsorber via Two-Step Surface-Initiated
 Molecular Imprinting Utilizing a Multi-Functional Polymeric Scaffold on a Macroporous
 Cellulose Membrane. RSC Adv. 2017, 7 (18), 11012–11019.
 https://doi.org/10.1039/C6RA28403E.
- Shang, Y.; Singh, P. R.; Chisti, M. M.; Mernaugh, R.; Zeng, X. Immobilization of a Human Epidermal Growth Factor Receptor 2 Mimotope-Derived Synthetic Peptide on Au and Its Potential Application for Detection of Herceptin in Human Serum by Quartz Crystal Microbalance. *Anal. Chem.* **2011**, *83* (23), 8928–8936. https://doi.org/10.1021/ac201430p.
- 13 (30) Leo, N.; Shang, Y.; Yu, J.; Zeng, X. Characterization of Self-Assembled Monolayers of 14 Peptide Mimotopes of CD20 Antigen and Their Binding with Rituximab. *Langmuir* **2015**, 15 31 (51), 13764–13772. https://doi.org/10.1021/acs.langmuir.5b02605.
- (31) Liu, J.; Chisti, M. M.; Zeng, X. General Signal Amplification Strategy for Nonfaradic
 Impedimetric Sensing: Trastuzumab Detection Employing a Peptide Immunosensor. *Anal. Chem.* 2017, 89 (7), 4013–4020. https://doi.org/10.1021/acs.analchem.6b04570.
- Liu, W.; Bennett, A. L.; Ning, W.; Tan, H.-Y.; Berwanger, J. D.; Zeng, X.; Bruening, M.
 L. Monoclonal Antibody Capture and Analysis Using Porous Membranes Containing
 Immobilized Peptide Mimotopes. *Anal. Chem.* 2018, 90 (20), 12161–12167.
 https://doi.org/10.1021/acs.analchem.8b03183.
- Liu, W.; Pang, Y.; Tan, H.-Y.; Patel, N.; Jokhadze, G.; Guthals, A.; Bruening, M. L.
 Enzyme-Containing Spin Membranes for Rapid Digestion and Characterization of Single
 Proteins. *Analyst* 2018, *143* (16), 3907–3917. https://doi.org/10.1039/C8AN00969D.
- Heat Inactivation of Serum https://www.gembio.com/post/heat-inactivation-serum (accessed Oct 16, 2020).
- Wang, C.; Yan, Q.; Liu, H.-B.; Zhou, X.-H.; Xiao, S.-J. Different EDC/NHS Activation
 Mechanisms between PAA and PMAA Brushes and the Following Amidation Reactions.
 Langmuir 2011, 27 (19), 12058–12068. https://doi.org/10.1021/la202267p.
- 31 (36) Dai, J.; Bao, Z.; Sun, L.; Hong, S. U.; Baker, G. L.; Bruening, M. L. High-Capacity
 32 Binding of Proteins by Poly(Acrylic Acid) Brushes and Their Derivatives. *Langmuir*33 **2006**, 22 (9), 4274–4281. https://doi.org/10.1021/la0600550.
- Jain, P.; Sun, L.; Dai, J.; Baker, G. L.; Bruening, M. L. High-Capacity Purification of His Tagged Proteins by Affinity Membranes Containing Functionalized Polymer Brushes.
 Biomacromolecules 2007, 8 (10), 3102–3107. https://doi.org/10.1021/bm700515m.
- Jain, P.; Baker, G. L.; Bruening, M. L. Applications of Polymer Brushes in Protein
 Analysis and Purification. *Annu. Rev. Anal. Chem.* 2009, 2 (1), 387–408.
 https://doi.org/10.1146/annurev-anchem-060908-155153.
- 40 (39) Kobayash, T.; Shibui, T. Isolation of Mimotopes to the Anti-Human VEGF Antibody
 41 Bevacizumab by MRNA Display Using Random Peptide Libraries and the Vaccination of
 42 a Rabbit. *Adv. Biosci. Biotechnol.* **2011**, *02*, 97. https://doi.org/10.4236/abb.2011.22015.
- (40) Wang, A.; Cui, M.; Qu, H.; Di, J.; Wang, Z.; Xing, J.; Wu, F.; Wu, W.; Wang, X.; Shen,
 L.; Jiang, B.; Su, X. Induction of Anti-EGFR Immune Response with Mimotopes
 Identified from a Phage Display Peptide Library by Panitumumab. *Oncotarget* 2016, 7
 (46), 75293–75306. https://doi.org/10.18632/oncotarget.12167.

- 1 (41) Perosa, F.; Favoino, E.; Vicenti, C.; Guarnera, A.; Racanelli, V.; Pinto, V. D.; Dammacco, F. Two Structurally Different Rituximab-Specific CD20 Mimotope Peptides Reveal That Rituximab Recognizes Two Different CD20-Associated Epitopes. *J. Immunol.* **2009**, *182* (1), 416–423. https://doi.org/10.4049/jimmunol.182.1.416.
- Takahashi, T. T.; Austin, R. J.; Roberts, R. W. MRNA Display: Ligand Discovery,
 Interaction Analysis and Beyond. *Trends Biochem. Sci.* 2003, 28 (3), 159–165.
 https://doi.org/10.1016/S0968-0004(03)00036-7.
- 8 (43) Mimmi, S.; Maisano, D.; Quinto, I.; Iaccino, E. Phage Display: An Overview in Context to Drug Discovery. *Trends Pharmacol. Sci.* **2019**, *40* (2), 87–91. https://doi.org/10.1016/j.tips.2018.12.005.
- 11 (44) Smith, G. P.; Scott, J. K. [15] Libraries of Peptides and Proteins Displayed on Filamentous 12 Phage. In *Methods in Enzymology*; Recombinant DNA Part H; Academic Press, 1993; 13 Vol. 217, pp 228–257. https://doi.org/10.1016/0076-6879(93)17065-D.
- (45) Hanes, J.; Plückthun, A. In Vitro Selection and Evolution of Functional Proteins by Using
 Ribosome Display. *Proc. Natl. Acad. Sci.* 1997, 94 (10), 4937–4942.
 https://doi.org/10.1073/pnas.94.10.4937.
- 17 (46) Nemoto, N.; Miyamoto-Sato, E.; Husimi, Y.; Yanagawa, H. In Vitro Virus: Bonding of
 18 MRNA Bearing Puromycin at the 3'-Terminal End to the C-Terminal End of Its Encoded
 19 Protein on the Ribosome in Vitro. *FEBS Lett.* **1997**, *414* (2), 405–408.
 20 https://doi.org/10.1016/s0014-5793(97)01026-0.
- 21 (47) Roberts, R. W.; Szostak, J. W. RNA-Peptide Fusions for the in Vitro Selection of Peptides
 22 and Proteins. *Proc. Natl. Acad. Sci.* 1997, 94 (23), 12297–12302.
 23 https://doi.org/10.1073/pnas.94.23.12297.
- Van Regenmortel, M. H. V. Antigenicity and Immunogenicity of Synthetic Peptides. *Biologicals* **2001**, *29* (3), 209–213. https://doi.org/10.1006/biol.2001.0308.
- 26 (49) Chu, K. H.; Hashim, M. A. Protein Adsorption on Ion Exchange Resin: Estimation of Equilibrium Isotherm Parameters from Batch Kinetic Data. *Biotechnol. Bioprocess Eng.* **2006**, *11* (1), 61–66. https://doi.org/10.1007/BF02931870.
- (50) Swenson, H.; Stadie, N. P. Langmuir's Theory of Adsorption: A Centennial Review.
 Langmuir 2019, 35 (16), 5409–5426. https://doi.org/10.1021/acs.langmuir.9b00154.
- Zhang, S.; Garcia-D'Angeli, A.; Brennan, J. P.; Huo, Q. Predicting Detection Limits of
 Enzyme-Linked Immunosorbent Assay (ELISA) and Bioanalytical Techniques in General.
 The Analyst 2014, 139 (2), 439–445. https://doi.org/10.1039/C3AN01835K.
- Smith, T. W.; Butler, V. P.; Haber, E. Characterization of Antibodies of High Affinity and Specificity for the Digitalis Glycoside Digoxin. *Biochemistry* **1970**, *9* (2), 331–337. https://doi.org/10.1021/bi00804a020.
- (53) Heinrich, L.; Tissot, N.; Hartmann, D. J.; Cohen, R. Comparison of the Results Obtained
 by ELISA and Surface Plasmon Resonance for the Determination of Antibody Affinity. *J. Immunol. Methods* 2010, 352 (1), 13–22. https://doi.org/10.1016/j.jim.2009.10.002.
- 40 (54) Karlsson, R.; Michaelsson, A.; Mattsson, L. Kinetic Analysis of Monoclonal Antibody 41 Antigen Interactions with a New Biosensor Based Analytical System. *J. Immunol.* 42 *Methods* 1991, 145 (1), 229–240. https://doi.org/10.1016/0022-1759(91)90331-9.
- 43 (55) Stanley, C.; Lew, A. M.; Steward, M. W. The Measurement of Antibody Affinity: A
 44 Comparison of Five Techniques Utilizing a Panel of Monoclonal Anti-DNP Antibodies
 45 and the Effect of High Affinity Antibody on the Measurement of Low Affinity Antibody.

- 1 J. Immunol. Methods 1983, 64 (1), 119–132. https://doi.org/10.1016/0022-1759(83)90390-2 3.
- (56) Friguet, B.; Chaffotte, A. F.; Djavadi-Ohaniance, L.; Goldberg, M. E. Measurements of the True Affinity Constant in Solution of Antigen-Antibody Complexes by Enzyme-Linked Immunosorbent Assay. *J. Immunol. Methods* 1985, 77 (2), 305–319. https://doi.org/10.1016/0022-1759(85)90044-4.
- 7 (57) Malmqvist, M. Surface Plasmon Resonance for Detection and Measurement of Antibody-8 Antigen Affinity and Kinetics. *Curr. Opin. Immunol.* **1993**, *5* (2), 282–286. 9 https://doi.org/10.1016/0952-7915(93)90019-O.
- 10 (58) Freyer, M. W.; Lewis, E. A. Isothermal Titration Calorimetry: Experimental Design, Data Analysis, and Probing Macromolecule/Ligand Binding and Kinetic Interactions. In *Methods in Cell Biology*; Biophysical Tools for Biologists, Volume One: In Vitro Techniques; Academic Press, 2008; Vol. 84, pp 79–113. https://doi.org/10.1016/S0091-679X(07)84004-0.
- (59) Mammen, M.; Choi, S.-K.; Whitesides, G. M. Polyvalent Interactions in Biological
 Systems: Implications for Design and Use of Multivalent Ligands and Inhibitors. *Angew. Chem. Int. Ed.* 1998, 37 (20), 2754–2794. https://doi.org/10.1002/(SICI)1521-3773(19981102)37:20<2754::AID-ANIE2754>3.0.CO;2-3.
- (60) Bilgiçer, B.; Moustakas, D. T.; Whitesides, G. M. A Synthetic Trivalent Hapten That
 Aggregates Anti-2,4-DNP IgG into Bicyclic Trimers. J. Am. Chem. Soc. 2007, 129 (12),
 3722–3728. https://doi.org/10.1021/ja067159h.
- 22 (61) Bilgiçer, B.; Thomas, S. W.; Shaw, B. F.; Kaufman, G. K.; Krishnamurthy, V. M.; Estroff, L. A.; Yang, J.; Whitesides, G. M. A Non-Chromatographic Method for the Purification of a Bivalently Active Monoclonal IgG Antibody from Biological Fluids. *J. Am. Chem. Soc.* 2009, 131 (26), 9361–9367. https://doi.org/10.1021/ja9023836.
- (62) Golay, J.; Semenzato, G.; Rambaldi, A.; Foà, R.; Gaidano, G.; Gamba, E.; Pane, F.; Pinto,
 A.; Specchia, G.; Zaja, F.; Regazzi, M. Lessons for the Clinic from Rituximab
 Pharmacokinetics and Pharmacodynamics. *mAbs* 2013, 5 (6), 826–837.
 https://doi.org/10.4161/mabs.26008.
- 30 (63) Ketzer, S.; Schimmel, K.; Koopman, M.; Guchelaar, H.-J. Clinical Pharmacokinetics and Pharmacodynamics of the Epidermal Growth Factor Receptor Inhibitor Panitumumab in the Treatment of Colorectal Cancer. *Clin. Pharmacokinet.* **2018**, *57* (4), 455–473. https://doi.org/10.1007/s40262-017-0590-9.
- 34 (64) Bevacizumab (Avastin®) https://www.ibl-america.com/bevacizumab/ (accessed Oct 21, 2020).
- 36 (65) Rituximab MAb-Based ELISA Assay | Rituxan Assay. Eagle Biosciences.
- 37 (66) Desvignes, C.; Passot, C.; Ternant, D.; Caulet, M.; Guérineau, C.; Lecomte, T.; Paintaud, G. Development and Validation of an ELISA to Study Panitumumab Pharmacokinetics.
 39 *Bioanalysis* **2018**, *10* (4), 205–214. https://doi.org/10.4155/bio-2016-0292.
- 40 (67) Min, J.; Nothing, M.; Coble, B.; Zheng, H.; Park, J.; Im, H.; Weber, G. F.; Castro, C. M.;
 41 Swirski, F. K.; Weissleder, R.; Lee, H. Integrated Biosensor for Rapid and Point-of-Care
 42 Sepsis Diagnosis. *ACS Nano* 2018, *12* (4), 3378–3384.
 43 https://doi.org/10.1021/acsnano.7b08965.

1 TOC Graphic

